Differential oxidation of APE1 suggests oxidation-associated modulation of endonuclease activity

Carson Gray[1], Gopikaashri Chidambaranathan[2], Nate Tolla[3], B. Mattingly[1], M. Daggett[1], S. Thomas[1], B. Freudenthal[4], and JF Treml[1†]

Apurinic/apyrimidinic endonuclease 1 (APE1) is an essential enzyme in the base excision repair (BER) pathway, hydrolyzing the phosphodiester backbone upstream of abasic sites. Beyond its canonical repair role, APE1 also acts as a redox-dependent regulator of multiple transcription factors, leading to its alternative designation, redox effector factor 1 (Ref-1). Given its dual roles in genome maintenance and transcriptional control, APE1 dysregulation has been strongly implicated in cancer and other diseases. When enacting its redox function, APE1 undergoes a redox cycling mechanism which has been proposed to involve the formation of intramolecular disulfide bonds. Of note, the nucleophilic cysteine is not solvent accessible, and the other redox active cysteine residues are too distant for covalent interaction in its native conformation. Consequently, a conformational shift may be required to accommodate the chemistry of substrate reduction. We propose that APE1's endonuclease role may be influenced by oxidation states that emerge from its function as a redox regulator, potentially leading to distinct redox-dependent functional states. To investigate this possibility, we exposed APE1 to mildly oxidizing conditions for various lengths of time and quantified its relative endonuclease activity. Interestingly, over a short period of H^2O^2 treatment, APE1 consistently exhibited higher relative endonuclease activity; however, longer periods of treatment resulted in inconsistent endonuclease activity across experimental groups. These results indicate that APE1 activity is associated with mild H^2O^2 treatment conditions and may increase under short exposure times, although oxidation state was not directly measured and conditions are inferred from prior studies of similar H^2O^2 exposure.

Oncogenesis arises due to a complex combination of interrelated factors, but frequently involves some form of DNA damage.1 One of the most prevalent sources of such damage is oxidative stress, which occurs when the generation of reactive oxygen species (ROS) exceeds the capacity of cellular antioxidant systems, resulting in the accumulation of reactive species that can damage nearby biomolecules, including DNA and proteins.2 These interactions can give rise to a variety of DNA lesions, including oxidized bases and abasic sites, which, if left unrepaired, can compromise genomic integrity and contribute to carcinogenesis.1,2

Cells possess sophisticated mechanisms by which they recognize and repair DNA damage. One such mechanism is the base excision repair (BER) pathway, which can accurately identify and replace singular damaged or incorrect nucleotides. In mammals, the damaged base is removed by a damage-specific glycosylase, followed by backbone hydrolysis by APE1 to generate a 3′-hydroxyl and an internal 5′-deoxyribose phosphate terminus, which is subsequently removed before the missing nucleotide is replaced by DNA polymerase β. Finally, DNA ligase III seals the nick at the 3' end of the new base.3 This pathway is vital to the development and survival of organisms, as evidenced by the blastocyst-stage lethality of murine APE1 knockout models.4 Furthermore, it has been found that loss of Ape1 after birth in the neural tissue of mice leads to the rapid and widespread development of brain tumors.5 Interestingly, APE1 is overexpressed in certain cancers, potentially serving a protective role, and there is interest in developing drugs that target APE1 for cancer treatment.6,7 Taken together, these observations suggest that APE1 has a complex and context-dependent role in cancer development. High-resolution structural and kinetic data demonstrate the specificity with which APE1 recognizes and cleaves its substrate, and it has been found that several pathological mutations of APE1 have the effect of reducing its endonuclease activity.8,9 Working towards a more complete understanding of the role of APE1 in oncogenesis is thus of high importance and relevance.

While APE1 has traditionally been associated with the BER pathway, it is also known to modulate the expression of several genes by reducing inactivating disulfide linkages in their transcription factors, including AP-1.10 APE1 enacts this function through a redox cycling mechanism that has been proposed to involve intramolecular disulfide bond formation; Cys65, acting as the nucleophilic cysteine, attacks one of the sulfur atoms involved in the substrate disulfide bond, leading to the formation of a mixed disulfide bond between APE1 and the substrate. To release the activated substrate, a resolving cysteine, potentially Cys93 or Cys99, may attack Cys65, allowing the substrate to dissociate and leaving

[1]University of Kansas, Edwards Campus, Biotechnology
[2]Washburn Rural High School
[3]Mill Valley High School
[4]University of Kansas Medical Center
[†]Corresponding Author jtreml@ku.edu

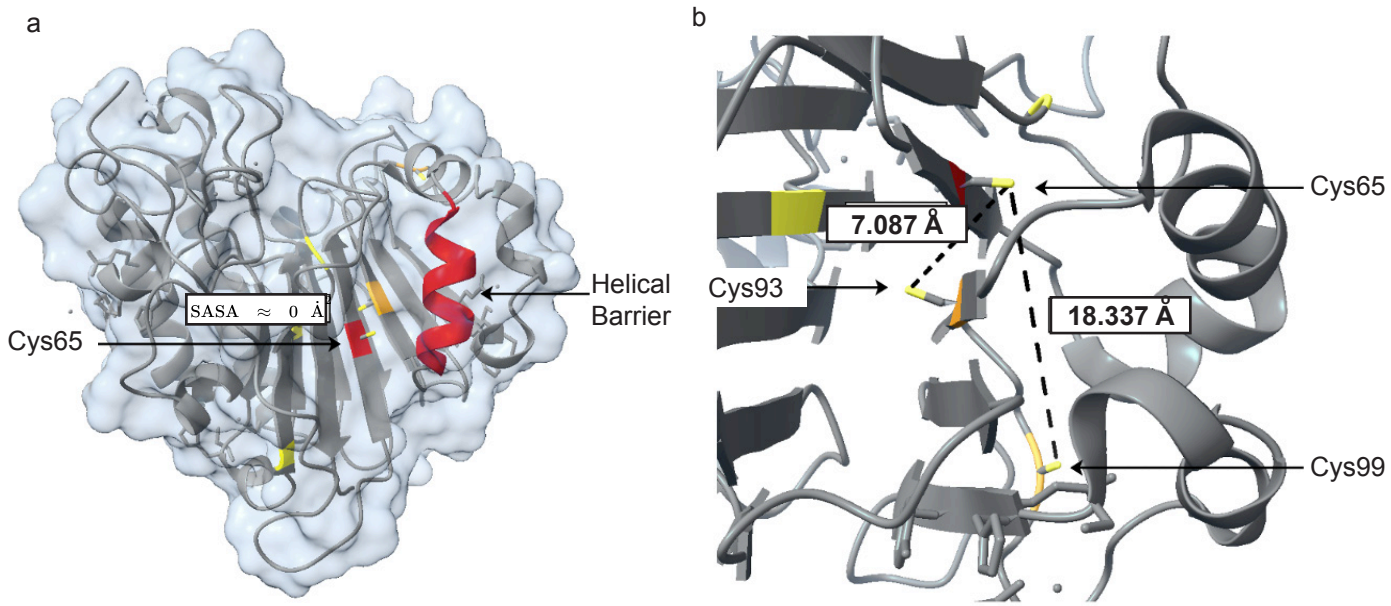

Figure 1 | APE1 Structure and Cystidine locations
(a) Characterization of Cys65 solvent accessibility and adjacent helical barrier.
(b) Distances between Cys65, Cys93, and Cys99

APE1 in an oxidized disulfide state.11,12 A growing body of research has demonstrated the multifunctionality of APE1 in regulating cellular physiology under oxidative stress, including mitochondrial function, neural survival, and cell cycle progression.13–15

In the native state of APE1, Cys65 is positioned within an interior β-sheet, with Cys93 located on the opposite side of the sheet face. Cys99 is located on a connecting loop relatively nearby. These structural features complicate mechanistic interpretations of its redox function, as Cys65 is not accessible to the solvent, and Cys93 and Cys99 are too distant to form covalent interactions with it. There is evidence to suggest that APE1 can assume a partially unfolded state, which may allow Cys65 to act as a nucleophile and form covalent interactions with the resolving cysteines.16 This suggests that APE1 may exist in an equilibrium between its native reduced form and alternate conformational states potentially associated with redox activity.

We hypothesized that APE1 may exhibit altered endonuclease kinetics under oxidizing conditions relative to untreated protein. Our data indicate that APE1 endonuclease activity is increased following short exposure to mildly oxidizing conditions, suggesting that APE1 activity may be correlated to its oxidation state. While oxidation state was not directly confirmed, we believe this work prompts further investigation into whether APE1 endonuclease activity is modulated by its redox-regulatory function.

Materials and Methods

Bacterial Expression of APE1

pET28HIS-hAPE1 was a gift from Primo Schaer (plasmid # 70757 ; http://n2t.net/addgene:70757 ; RRID:Addgene_70757), which was used to produce His-tagged APE1 in a bacterial expression system. Kanamycin (K1377-1G, Sigma-Aldrich) used at a working concentration in all media at 50 µg/mL. All bacterial cultures were grown in Luria–Bertani (LB, 12780052, Invitrogen) broth or agar supplemented with kanamycin unless otherwise specified. Individual bacterial colonies were inoculated into 10 mL LB medium containing kanamycin and incubated at 37 °C with shaking (200 rpm) for 3–5 h. For larger starter cultures (10–40 mL), a single colony was inoculated and incubated for 4–6 h. Cultures were grown to an optical density at 600 nm (OD_{600}) of 0.55–0.6; growth beyond this point was avoided to ensure optimal protein expression. One milliliter of each culture was centrifuged at 16,000 x g for 5 min, and the resulting cell pellet was stored at –20 °C. The remaining culture was either used immediately for inoculation of expression cultures or stored at 4 °C overnight.

Starter cultures were used to inoculate larger expression cultures in LB medium containing kanamycin, using the following ratios: 1 mL starter culture per 50 mL, 5 mL per 250 mL, and 20–40 mL per 1–1.5 L culture. Cultures were incubated with shaking at 37 °C until reaching an $OD_{600)}$ of 0.5–0.6.

Expression was induced with 0.5 mM isopropyl β-D-1-thiogalactopyranoside (IPTG, 15529019, Invitrogen) at 20 °C and incubated for 12–18 h with shaking.

Cells were harvested by centrifugation at 3,500 × g for 20 min at 4 °C and either processed immediately or stored at –20 °C.

Cell pellets were resuspended in His-tag lysis buffer [50 mM Tris–Cl (pH 8.0), 1 mM imidazole, 100 mM NaCl, 0.1 mM EDTA] at a ratio of 2–10 mL buffer per 20–100 mL of culture, 10–25 mL buffer per 100–500 mL, or 25–50 mL buffer per 1–2 L culture. Immediately prior to use, phenylmethylsulfonyl fluoride (PMSF, AB14103210G, Abcam) was added to 1 mM and β-mercaptoethanol(21985023, Gibco) to 10 mM.

Cells were lysed by addition of lysozyme to a final concentration of 0.5–1 mg/mL, followed by incubation on ice for 30 min with gentle mixing. Samples were sonicated on ice (3 × 2 min bursts) and centrifuged at 15,000 × g for 20 min at 4 °C. The supernatant was filtered (0.45 µm) and used for affinity purification.

Nickel–nitrilotriacetic acid (Ni–NTA, PI88221, ThermoScientific) resin was gently resuspended, and 1–2 mL of slurry was added to a chromatography column. The resin was equilibrated by washing with 5 column volumes (CV) of water, followed by 5–10 CV of lysis buffer. Clarified lysate

was applied to the column and allowed to pass through by gravity. The resin was washed with 10 CV of wash buffer [50 mM Tris–Cl (pH 8.0), 300 mM NaCl, 10 mM imidazole, 0.1 mM EDTA, and 1 mM PMSF].

Bound protein was eluted with 5 CV of elution buffer [50 mM Tris–Cl (pH 8.0), 50 mM NaCl, 300 mM imidazole, 0.1 mM EDTA, and 1 mM PMSF]. Eluted fractions were analyzed by SDS–PAGE, and fractions containing APE1 were pooled. Imidazole was removed by dialysis against storage buffer [50 mM NaCl, 1 mM dithiothreitol (DTT), 0.05 mM EDTA, and 10% glycerol].

Dialysis tubing was pre-equilibrated in buffer (50 mM Tris–HCl, pH 8.0, 100 mM NaCl). Samples were dialyzed against 100 volumes of replacement buffer at 4 °C with three buffer changes over ~20 h (2 h, 2 h, and overnight). Protein concentration was determined by spectrophotometry, and samples were concentrated to 2–3 mg/mL.

Preparation of Duplex DNA Substrates

Oligonucleotides were stored at 100 µM in TE buffer (10 mM Tris–HCl, 1 mM EDTA, pH 8.0). For duplex formation, complementary oligonucleotides were mixed to final concentrations of 12 µM (template) and 10 µM (FAM-labeled THF abasic construct, ThermoScientific) in TE buffer. Samples were annealed by heating to 98 °C and cooled to 25 °C at 1 °C/min in a thermal cycler. Aliquots were frozen at -20 °C for later use.

Controlled Oxidation and Endonuclease Digestion

Reactions were performed in 2x base excision repair (BER) buffer [40 mM HEPES–KOH (pH 7.5), 100 mM KCl, 10 mM $MgCl_2$, 0.1 mg/mL bovine serum albumin]. Hydrogen peroxide (1 mM final; 0.034% w/w) was freshly prepared from a 30% stock.

Reactions were performed in 2x base excision repair (BER) buffer [40 mM HEPES–KOH (pH 7.5), 100 mM KCl, 10 mM $MgCl_2$, 0.1 mg/mL bovine serum albumin]. Hydrogen peroxide (1 mM final; 0.034% w/w) was freshly prepared from a 30% stock.

Purified APE1 (10 µM) was pre-incubated with 1 mM H_2O_2 for 0, 5, 15, or 30 minutes at room temperature. Following oxidation, excess H_2O_2 was quenched with catalase prior to activity assays. 10 µL duplex DNA (400 nM) was mixed with 20 µL 2X BER buffer. 10 µL of APE1 (20 nM) was added to each reaction, and the mixture was incubated at 37 °C for 8 minutes before being quenched with 40 µL of 0.5 M EDTA at pH 8 and placed on ice. For each run, an additional reaction was prequenched for a negative control, and another was allowed to go to completion (40 minutes). 160 µL of loading dye (98% formamide, 0.25 mg/mL bromophenol blue) was added to each sample before proceeding to electrophoresis.

Denaturing PAGE and Detection

Reactions were analyzed by polyacrylamide gel electrophoresis (PAGE) using 20% denaturing gels containing 8 M urea in 1× TBE buffer. Prior to loading, the gels were pre-run at 300 V for 30 minutes, each lane was syringe-rinsed with 1x TBE, and samples were heated to 85 °C for 4.5 min and snap-chilled on ice.

Electrophoresis was performed at 300 V until the bromophenol blue dye front reached approximately 80% of the gel length (~1.5 hours). The gels were gently agitated in 1X TBE for 30 minutes before analysis. Band intensities were quantified by densitometry using a LI-COR imaging system.

Kinetic Data Analysis and Statistical Significance

When analyzing the kinetics gels, three bands were present. Substantial evidence suggested that the two bands with the lowest electrophoretic mobility corresponded

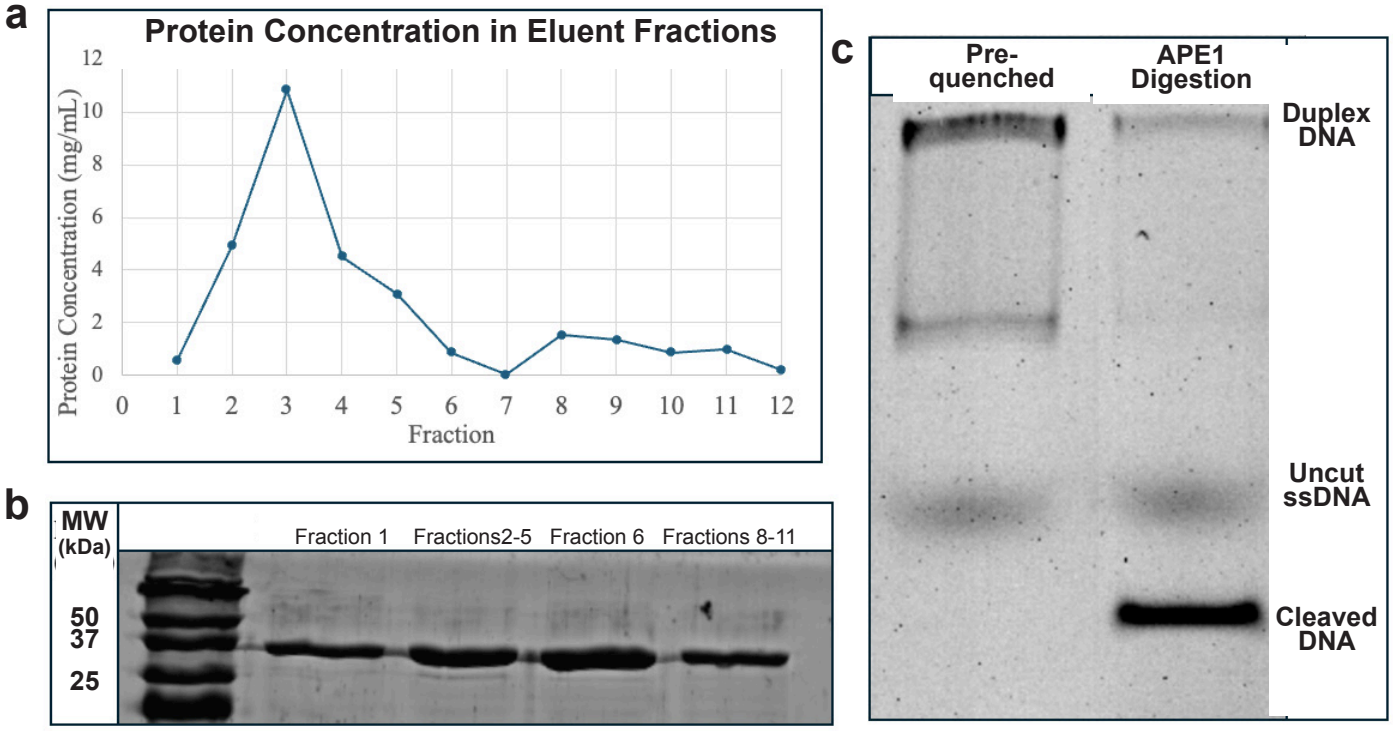

Figure 2 |APE1 Purification. (a) Concentration of APE1 fractions eluted from affinity column as determined by absorbance at 280 nm. (b) Coomassie-stained SDS-PAGE gel showing samples from fraction 1, fraction 6, and grouped samples of fractions 2-5 and 8-11. (c) PAGE gel of FAM-labeled DNA pre-quenched versus APE1 digested.

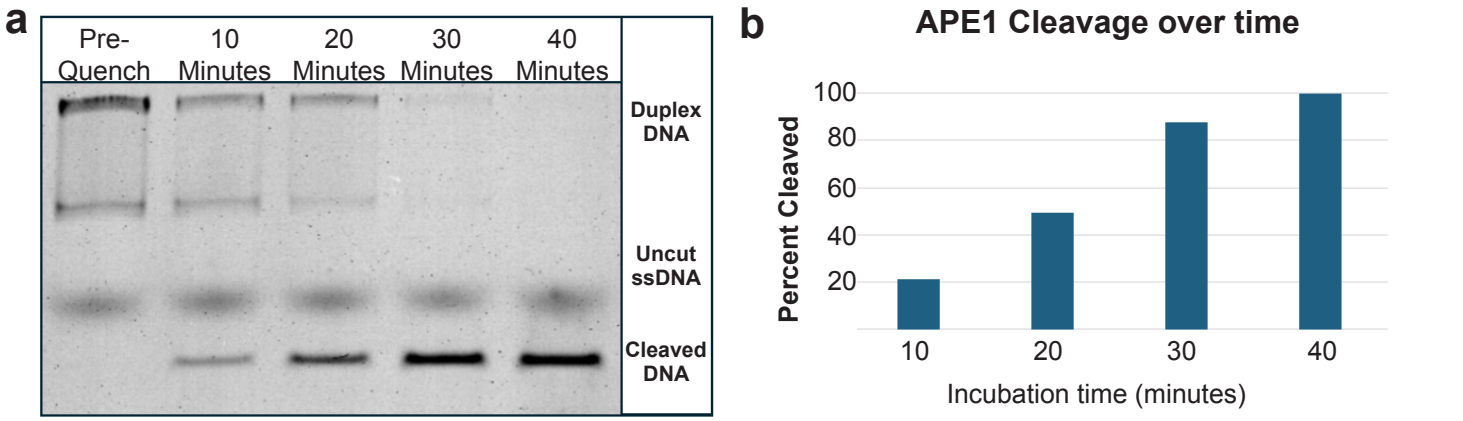

Figure 3 | APE1 Cleavage over Time. (a) Denaturing DNA PAGE of duplexed FAM-labelled oligos incubated with APE1 for various time points. The highest band is believed to be uncut duplex DNA, the middle band single stranded uncut DNA, and the bottom-most band cleaved single-stranded DNA. (b) Percent cleavage of APE1 digestion time points.

to single-stranded or duplex uncut FAM-labeled oligonucleotides, while the band of highest electrophoretic mobility corresponded to single-stranded cleaved oligonucleotides. For gel quantification, band intensities were measured using defined regions of interest (ROIs) corresponding to cleaved and uncleaved species, with identical ROIs applied across all lanes for consistency. Background signal was estimated from equivalent ROIs in regions lacking specific bands and subtracted from corresponding experimental intensities. The intensities of the uncleaved and cleaved ROIs was used to determine total signal, and the proportion of cleaved substrate was calculated as the cleaved intensity divided by the sum of cleaved and uncleaved intensities. This value was then normalized to the corresponding non-oxidized control to obtain relative activity. Statistical significance was assessed using a one-sample t-test comparing normalized relative activity values to an expected mean of 1, with p-values calculated using Microsoft Excel. The t-statistics were obtained using the standard one-sample t-test equation, where n represents the number of independent experimental replicates:

$$t = \frac{\bar{x} - 0.1}{S/\sqrt{n}}$$

Results

APE1 Expression

APE1 was expressed in a bacterial system and purified using Ni-based chromatography. Purified fractions were analyzed using PAGE, and concentrations were determined spectrophotometrically. All tested fractions produced bands indicating a protein with a molecular weight slightly less than 37 kDa, which is consistent with APE1 (Mr = ~35.5 kDa).

To ensure that the purified APE1 was catalytically active, a THF abasic analogue-containing FAM-labelled duplex DNA strand was incubated at 100 nM with 5 nM APE1 at 37 °C for 40 minutes. This was compared to a prequenched solution containing the same components. Of the three bands present, the two with lower electrophoretic mobility decreased as the intensity of the higher-mobility band increased . The uncut DNA may not fully denature under the given conditions, leading to the formation of two bands; however, because the bands disappear after longer incubations (See **Fig. 2**), the cut DNA is likely to fully denature.

Estimation of Enzyme Kinetics

An identical reaction was quenched after varied lengths of incubation to establish the period of kinetic linearity. The time points tested were 10, 20, 30, and 40 minutes. The reaction appeared to reach completion by 40 minutes, and cleavage appeared to be approximately linear within the 0–30-minute range. To ensure that the enzyme maintained constant velocity, 8 minutes was chosen to be the experimental incubation time for comparison across differentially oxidized species. The APE1-dependence of results and quenching efficacy was established using a prequench control and a fully cleaved control were included in every experiment.

APE1 was incubated in hydrogen peroxide for 0, 5, and 15 minutes before being quenched with catalase. After incubation with the model substrate, reactions were quenched and subjected to denaturing PAGE. FAM-based fluorescent intensity was quantified at regions of interest corresponding to uncut and cut fragments. Cleavage percentages were calculated for all groups and were normalized to the 0-minute oxidation control. A statistically significant increase in endonuclease activity was observed following 5 minutes of H_2O_2 treatment, while there was no significance found in the 30-minute group (n = 3).

Jurkat E6.1 T cells experience quantitatively different signaling after exposure to acidic environments

Exceaqui dolor aliqui to conem doluptisimi, ex es debita volorpo resedia porumet ut acepel ipsam vene laut min pedi delestium volorum es comnis eos quo tetur?

Axim et vendes si quas se latquidis doluptas net exerio. Nequia volori dolut eos excea ea solorum quiam, sam, sequae alibus, con culles volupta tincta cullupt atquatus exceatur serferferro deliqui omnisi id ma explign iendus utem fuga. Namet aut adis quamus enimo doluptia voluptatem net officaeri non nihicidem ipsanducium verumet autem inis most quod quae volupid utecepro et alia corecte dolorporro veles resto blacers pelluptaquia quunt alita endunto occab ium a quatem quas dolorionet officiam voloritae et harumqui sa quo culpa non ressequo comnien imusdam et, sim

Discussion

Fractions collected during APE1 purifications all exhibited a band corresponding to

APE1's molecular weight, suggesting that APE1 was successfully purified from the bacterial expression system. After dialysis, the solution was tested for APE1 endonuclease activity by adding a FAM-labeled THF-analogue model substrate. When the products were run by PAGE the solution was found to produce cleaved substrate. Furthermore, percent cleavage increased with incubation time prior to an EDTA quench, suggesting that the system is time-dependent and reliably quantifiable. Taken together, these results suggest that we were able to successfully purify active APE1 and could quantify its endonuclease activity.

When the endonuclease activity of H_2O_2-treated APE1 was compared with that of untreated APE1, the 5-minute time group consistently exhibited a roughly 20% increase in activity compared to the untreated APE1. This was surprising, as most enzymes tend to become less active in oxidizing conditions. However, since APE1 experiences oxidation because of its canonical redox activity, these results may reveal oxidation-dependent regulation of APE1 function. Specifically, APE1's endonuclease activity may be enhanced under mildly oxidizing conditions. We speculate that this effect may be related to its physiological redox states. Although the redox state of APE1 was not directly measured, our conditions were based on previous work that analyzed disulfide formation over time using tandem MS/MS.17 While still speculative, this would be consistent with the increased biological need for DNA repair due to oxidation-related accumulation of nucleotide damage.

Because APE1's redox state was not directly measured and residual DTT was present, the redox environment may have differed among groups. Furthermore, H_2O_2 may impact protein structure and DNA binding through mechanisms independent of specific cysteine oxidation. Given these limitations, Further work is needed to confirm APE1 oxidation state and determine its relationship to endonuclease activity . While limited in scope, these results may provide early evidence for an unexplored aspect of APE1 biology.

Future Directions

As noted throughout this manuscript, our work was limited by the inability to directly measure oxidation state alongside the observed changes in endonuclease kinetics. The most important next step would be to couple the kinetics assay with a method to directly assess APE1 redox state (e.g., thiol-specific labeling or mass spectrometry-based oxidation mapping). Direct measurement would resolve this important source of uncertainty in future work. Additionally, even if a relevant redox state was definitively connected to altered endonuclease activity, this does not necessarily establish biological relevance. If the change is only moderate, or if the rate of another step dominates the overall rate of BER, it may not influence DNA repair. To establish physiological relevance, an inhibitor specific to APE1's redox function (without affecting endonuclease activity) could be used to assess changes in DNA repair efficiency in vitro.

Author's Biography

Carson Gray is passionate about the molecular basis of biology, with a particular interest in the structure and physics of biomolecules. He has been admitted to the IGPBS program at KU Medical Center, where he plans to obtain his PhD in biochemistry or a related field.

Author Contributions

C.G. contributed to the design & execution of the work and wrote the manuscript. G.C. contributed to the protein structure figures and and related work. N.T. contributed to enzyme kinetics and related work. B.M.,, M.D., S.T., B.F., and J.T. contributed mentorship and reagents.

References

1. Basu, A. K. DNA Damage, Mutagenesis and Cancer. Int. J. Mol. Sci. 19, 970 (2018).
2. Kaur, R., Kaur, J., Mahajan, J., Kumar, R. & Arora, S. Oxidative stress—implications, source and its prevention. Environ. Sci. Pollut. Res. 21, 1599–1613 (2014).
3. Whitaker, A. M., Schaich, M. A., Smith, M. S., Flynn, T. S. & Freudenthal, Bret. D. Base ex-cision repair of oxidative DNA damage: from mechanism to disease. Front. Biosci. Landmark Ed. 22, 1493–1522 (2017).
4. Xanthoudakis, S., Smeyne, R. J., Wallace, J. D. & Curran, T. The redox/DNA repair protein, Ref-1, is essential for early embryonic development in mice. Proc. Natl. Acad. Sci. 93, 8919–8923 (1996).
5. Dumitrache, L. C. et al. Apurinic endonuclease-1 preserves neural genome integrity to maintain homeostasis and thermoregulation and prevent brain tumors. Proc. Natl. Acad. Sci. 115, E12285–E12294 (2018).
6. Fishel, M. L. et al. Knockdown of the DNA repair and redox signaling protein Ape1/Ref-1 blocks ovarian cancer cell and tumor growth. DNA Repair 7, 177–186 (2008).
7. Caston, R. A. et al. The multifunctional APE1 DNA repair–redox signaling protein as a drug target in human disease. Drug Discov. Today 26, 218–228 (2021).
8. Freudenthal, B. D., Beard, W. A., Cuneo, M. J., Dyrkheeva, N. S. & Wilson, S. H. Capturing snapshots of APE1 processing DNA damage. Nat. Struct. Mol. Biol. 22, 924–931 (2015).
9. Whitaker, A. M., Stark, W. J., Flynn, T. S. & Freudenthal, B. D. Molecular and structural char-acterization of disease-associated APE1 polymorphisms. DNA Repair 91–92, 102867 (2020).
10. Evans, A. R., Limp-Foster, M. & Kelley, M. R. Going APE over ref-1. Mutat. Res. Repair 461, 83–108 (2000).
11. Kelley, M. R., Georgiadis, M. M. & Fishel, M. L. APE1/Ref-1 Role in Redox Signaling: Translational Applications of Targeting the Redox Function of the DNA Repair/Redox Protein APE1/Ref-1. Curr. Mol. Pharmacol. 5, 36–53 (2012).
12. Frossi, B. et al. Endonuclease and redox activities of human apurinic/apyrimidinic endonucle-ase 1 have distinctive and essential functions in IgA class switch recombination. J. Biol. Chem. 294, 5198–5207 (2019).
13. Wang, Y.-T., Tzeng, D.-W., Wang, C.-Y., Hong, J.-Y. & Yang, J.-L. APE1/Ref-1 prevents oxi-dative inactivation of ERK for G1-to-S progression following lead acetate exposure. Toxicolo-gy 305, 120–129 (2013).
14. Li, M. et al. Human AP endonuclease/redox factor APE1/ref-1modulates mitochondrial func-tion after oxidative stress by regulating the transcriptional activity of NRF1. Free Radic. Biol. Med. 53, 237–248 (2012).
15. Vasko, M. R., Guo, C. & Kelley, M. R. The multifunctional DNA repair/redox enzyme Ape1/Ref-1 promotes survival of neurons after oxidative stress. DNA Repair 4, 367–379 (2005).
16. Su, D. et al. Interactions of Apurinic/Apyrimidinic Endonuclease with a Redox Inhibitor: Evi-dence for an Alternate Conformation of the Enzyme. Biochemistry 50, 82–92 (2011).
17. Luo, M. et al. Characterization of the Redox Activity and Disulfide Bond Formation in Apuri-nic/Apyrimidinic Endonuclease. Biochemistry 51, 695–705 (2012).

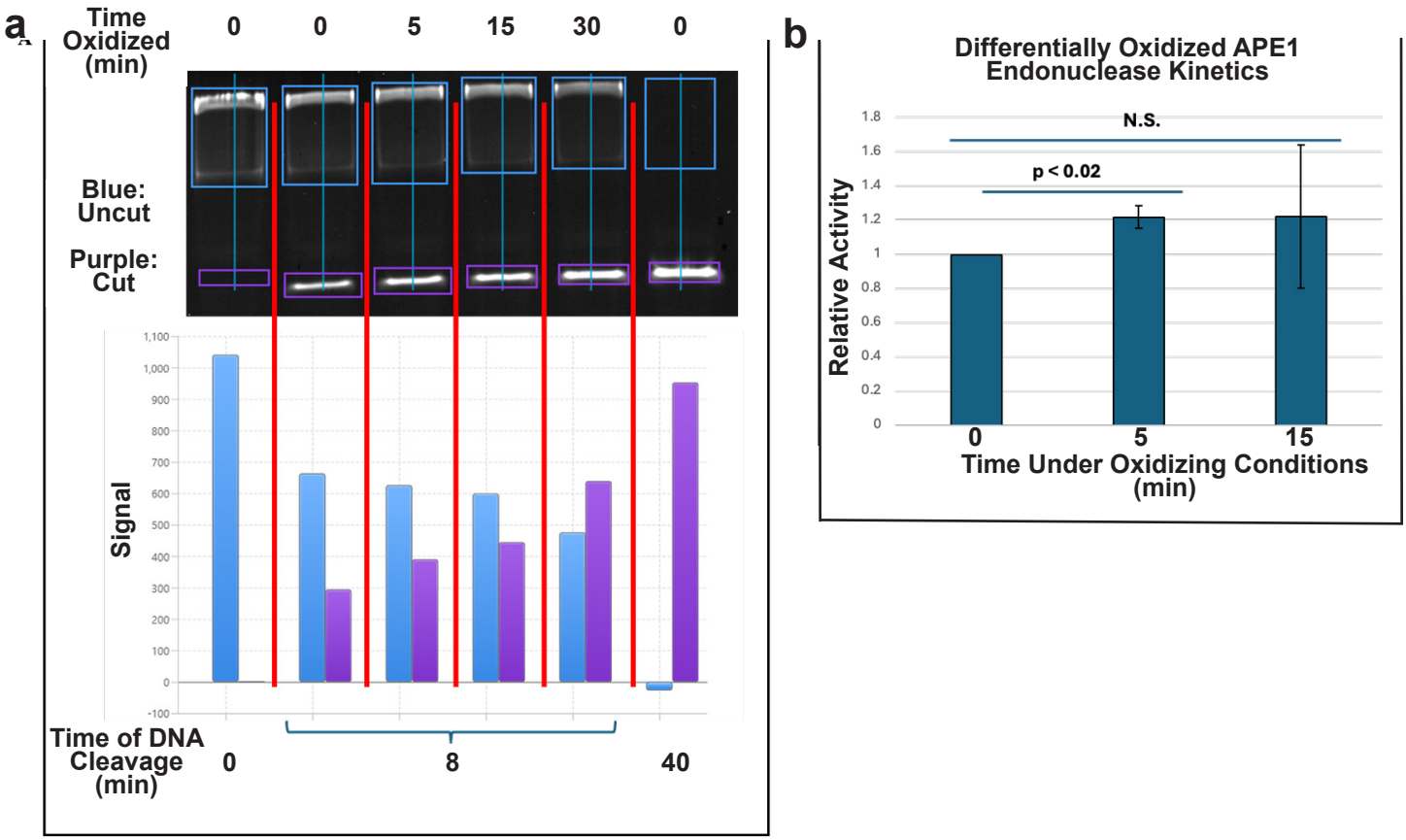

Figure 4 | Enzyme Kinetics. a Representative image of kinetics data showing AOI for uncut (blue) and cut (purple) DNA fragments. Fluorescent signal of these bands were first used to calculate percent cleavage, and were compared to the 0 min oxidized 8 min cleaved control to determine relative activity. **b** Relative activity of APE1 oxidized for 0, 5, and 15 min. 5 min oxidized APE1 exhibited a statistically significant enhancement of endonuclease activity ($p < 0.01$), while 15 min oxidized APE1 lacked statistical significance.